International Journal of Engineering Trends and Technology
ISSN: 2231–5381 / https://doi.org/10.14445/22315381/IJETT-V72I5P106

Volume 72 Issue 5, 51-57, May 2024

Original Article

Interaction of External Surface Cracks on Thick Cylinders under Mode III Moment and Combined with Mode I Loading

Al-Moayed, O.M.[1], Al Emran Ismail[2], Kareem, Ali K.[3]

[1]*Renewable Energy Research Center, University of Anbar, Iraq.*
[2]*Faculty of Mechanical and Manufacturing Engineering, Universiti Tun Hussein Onn Malaysia, Batu Pahat, Johor, Malaysia.*
[3]*Department of Biomedical Engineering, Al-Mustaqbal University College, Hillah, Iraq.*

[2]*Corresponding Author : emran@uthm.edu.my*

Received: 12 October 2023 Revised: 23 February 2024 Accepted: 04 May 2024 Published: 26 May 2024

Abstract *- Thick-walled cylinder is widely used in modern engineering and applications and they are used to withstand high internal and external pressure. Sometimes, it is used to transmit power from one to another points which is generally subjected to torsion or mode III moments. Under certain circumstances, external cracks are formed due to corrosion and material defects, which lead to premature failure. In this paper, ANSYS finite element analysis software is used to construct the cracks on the surface of thick cylinders under mode III and combined mode I and III loading conditions. Various crack geometries and configurations are used, such as crack aspect ratios, a/c = 0.4, 0.6, 0.8, 1.0 and 1.2 and relative crack depth, a/t = 0.2, 0.5 and 0.8. For parallel cracks, different relative distances, s/L is used, such as 0.004, 0.008, 0.016 and 0.032. According to the numerical results, if the number of cracks is more than two, the SIFs decrease when compared with a single crack. In terms of crack interactions, as expected, the degree of interaction is diminished when the cracks are away from each other. Also, it is shown that crack interaction influence for parallel cracks is demonstrated by shielding interaction influence only, while both shielding and amplification impacts are produced for non-coplanar cracks. The crack separation distance (horizontal and angular) between the cracks displayed substantial influence on interaction since it exhibited the ability to convert the interaction behavior from shielding to amplification impact (for angular).*

Keywords *- Crack interactions, Surface crack, Thick cylinder, Finite Element Analysis.*

1. Introduction

Thick cylinders subjected to torsional loading are commonly encountered in various engineering applications, such as rotating shafts, gears, and turbine components. However, these components are susceptible to the initiation and growth of surface cracks, which can have a detrimental effect on their structural integrity and lead to catastrophic failures. Understanding the behavior of surface cracks and their interactions in thick cylinders under torsion is of paramount importance for ensuring the safe and reliable operation of these critical systems. Several factors influence the surface crack interactions in thick cylinders under torsional loading. The crack geometry, including crack length, depth, orientation, and location, plays a crucial role in determining the stress concentration at the crack tip and the severity of crack interactions. The material properties, such as fracture toughness, shear modulus, and yield strength, also significantly influence crack propagation behavior and the ability of the material to resist crack growth. Extensive research has been conducted to investigate and understand the complex interactions between surface cracks in thick cylinders under torsion. Experimental studies, analytical models, and numerical simulations have been employed to explore various aspects of crack behavior, including crack initiation, propagation, coalescence, and branching. These studies have provided valuable insights into the mechanics of crack interactions and have contributed to the development of design guidelines and mitigation strategies for preventing failures in torsionally loaded engineering structures.

Moghaddam et al. [1] determined the Stress Intensity Factor (SIF) under mixed mode loading of functionally graded hollow cylinders. For this crack configuration under pure torsion, the mode II SIF follows the same trend as the mode I SIF as described above. On the other hand, for the mode III SIF, the peak value is always attained at the deepest point along the crack front, and it decreases as the gradation of modulus of elasticity increases. A similar dependency of the SIFs on material gradation was observed for a surface crack located at the outer surface of the cylinder. At the same time,

Fahem et al. [2] investigated the SIFs of cylindrical specimens under torsion moment. The geometry factor was inversely obtained from the stress intensity factor calculated through the finite element analysis to obtain a closed-form expression for K_I. To get the closed-form expression for K_I the geometry factor was formulated into two multiplicative functions, like Benthem equations, and the corresponding functions are obtained from the FE results for a range of specimen geometries. In terms of crack interaction, Zhu et al. [3] studied void or defect interactions under mode I, II and III loading.

The void rotation seems to follow the void growth mechanism with a shift from void-by-void rotation to multiple void rotations as the initial void volume fraction increases. However, this is highly dependent on the mode mixity ratio, with large ratios favouring multiple void rotations. The introduced mode III loading is found to favour a shift from multiple void interactions towards void-by-void growth for the largest initial void volume fraction as well as the highest mode mixity ratio considered. In the same fashion, a shift from multiple voids rotation towards void-by-void rotation is predicted. Several other research works can be found elsewhere [4-11]. In the case of crack interactions, especially on thick cylinders, the number of publications is insignificant, and a tremendous number of works are available, especially for single cracks [12-20].

Based on the literature, it is found that it the difficulty to find surface crack interactions on thick cylinders. Therefore, this work numerically investigates the behaviours of the parallel of two surface cracks to study the interactions under the torsion moment. ANSYS finite element analysis is used to model and solve the problems related to the crack interactions. The stress intensity factors of single and double cracks are determined, and the factor of crack interaction is calculated.

2. Determination of Stress Intensity Factors

In the present work, since the problem is considered in the LEFM region, the SIFs are assumed as the driving force for the interaction between the cracks; thus, it is essential to explain the methods utilized by Ansys to calculate the SIFs. In Ansys, there are two methods to determine the SIFs: (1) Displacement Extrapolation Method (DEM) AND (2) Interaction Integral Method (IIM). In the DEM, the SIFs are determined by describing the displacement between two nodes placed along the crack faces surrounding the crack tip.

While in the IIM for the SIFs computation uses area integration for 2-D problems and volume integration for 3-D problems. However, the IIM, compared to DEM, presents better precision, less mesh obligation and is easy to use. Therefore, in the present study, IIM was selected to calculate the SIFs. The interaction integral is described as [21]:

$$I_o = \frac{-\int_v q_{ij}\left(\sigma_{kl}\varepsilon_{kl}^{aux}\delta_{ij} - \sigma_{kj}^{aux}u_{ki} - \sigma_{kj}\varepsilon_{kj}^{aux}\right)dV}{\int_s \delta q_n ds \sigma_{ij}} \quad (1)$$

Where σ_{ij}, ε_{ij}, u_i are the stress, strain, and displacements, respectively. While σ^{aux}, ε^{aux}, u^{aux} are the stress, strain, and displacement of the auxiliary field, and q_i is the crack extension vector. Then, the interaction integral is correlated with the SIFs as [21]:

$$I = \frac{2}{E^*}(k_1 k_2^{aux} + k_2 k_2^{aux}) + \frac{1}{\mu}(k_3 k_3^{aux}) \quad (2)$$

Where ki (i = 1, 2, 3) represents SIFs for modes I, II and III, k_i^{aux} (i=1, 2, 3) denotes auxiliary mode I, II and III SIFs, E*=E for plane stress and E*=E/(1-v^2) for plain strain, E is the modulus of elasticity, v is Poisson's ratio, and μ is the modulus of rigidity.

3. Materials and Methods

In this work, thick hollow cylinders are considered, and it is to have an external surface crack, which is then subjected to torsion moment and combined with mode I loading. It is assumed that the external diameter is 250 mm with a wall thickness of 25 mm, which meets the criterion of a thick cylinder. The schematic diagram of the crack is revealed in Figure 1. The crack aspect ratio, a/c considered are 0.4, 0.6, 0.8, 1.0 and 1.2. While, the second parameter is relative crack depth, a/t equal to 0.2, 0.5 and 0.8. ANSYS Workbench software is used to construct a finite element model. The cracks take semi-elliptical shapes as in Figures 2(a) and 2(b) show the finite element model for the whole cylinder with the enlarged area of single and parallel cracks in the respective Figures 2(c) and 2(d). One end of the cylinder is fixed in all degrees of freedom, and at the other end torsion moment is applied remotely. In ANSYS software, the stress intensity factor is based on the interaction integral method, and they are normalized according to equations (3) and (4) for tension force and bending moment:

$$F_{Tor-II} = \frac{K_{II,cal,Tor}}{\tau\sqrt{\frac{\pi a}{Q}}_{max}} \quad (3)$$

$$F_{Tor-III} = \frac{K_{III,cal,Tor}}{\tau\sqrt{\frac{\pi a}{Q}}_{max}} \quad (4)$$

Where F_{Tor-II} and $F_{Tor-III}$ are the normalized SIFs for modes II and III under remote torsion loading, respectively. On the other hand, $K_{II,\,cal,\,Tor}$ and $K_{III,\,cal,\,Tor}$ are the calculated SIFs for modes II and III under torsion loading. While τ_{max} is the maximum shear stress, which is given by:

$$\tau\frac{TR_o}{J}_{max} \quad (5)$$

Where T is the applied torque, Ro is the outer radius of the hollow cylinder, and J is the polar moment of inertia, which is given for a hollow cylinder by:

$$J = \frac{\pi}{32}(D_o^4 - D_i^4) \quad (6)$$

Furthermore, in the case of mixed-mode loading, where the tension and bending were combined with torsion and applied remotely to the hollow cylinder.

Table 1. Comparison of SIFs for a single circumferential crack in a thick cylinder under tension

a/c =0.6	Deepest point			Surface point		
	a/t					
	0.2	0.5	0.8	0.2	0.5	0.8
Reference [84]	1.101	1.178	1.285	0.933	1.071	1.285
Present	1.074	1.160	1.243	0.911	0.1027	1.243
Error (%)	2.45	1.52	3.26	2.35	4.10	3.26
a/c =0.8	Deepest point			Surface point		
	a/t					
	0.2	0.5	0.8	0.2	0.5	0.8
Reference [84]	1.058	1.103	1.157	1.053	1.156	1.333
Present	1.048	1.114	1.161	1.034	1.161	1.366
Error (%)	0.94	-0.99	0.34	1.80	-0.43	-2.47

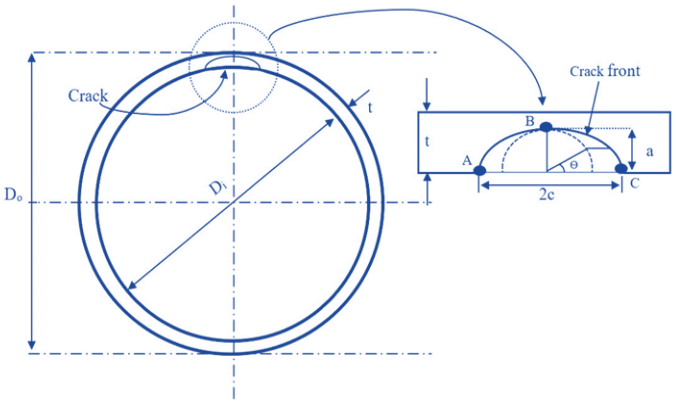

Fig. 1 Schematic diagram of surface crack

Due to this type of loading, SIFs for all three modes were calculated, and then each mode was normalized separately. Finally, the normalized SIFs are given by equivalent SIFs, F_{EQV}, because of the combined load, that is:

$$F_{EQV} = \sqrt{(F_I)^2 + (\lambda F_{II})^2 + \left(\frac{\lambda F_{III}}{1-\nu}\right)^2} \quad (7)$$

Where F_I, F_{II}, and F_{III} are the normalized SIFs for each mode under mixed-mode loading and is a ratio given by:

$$\lambda = \frac{\tau}{\sigma_b} \quad (8)$$

Where σ_b is a bending stress due to the bending moment. Finally, the normalized SIFs distribution is presented along the crack front as a function of the normalized crack front position. It is possible to define any point located on the crack front by using a non-dimensional coordinate named the normalized crack front position.

The utilized formula to normalize the position is 2Θ/π, where Θ is the parametric angle of the crack. Therefore, when 2Θ/π = (-1or 1), this value represents surface points (the point where the crack intersects the cylinder surface), while 2Θ/π =0, denoting the deepest point on the crack front. The interaction factor Ψ is defined as the ratio of the SIFs for the case of two cracks to the SIFs of a single crack; therefore, the following expression is used to determine the interaction factor [22]:

$$\Psi = \frac{F_{two-crack}}{F_{single\_crack}} \quad (9)$$

Where F_{two} cracks represent the normalized SIFs for the case of two cracks for any mode and type of loading, and F_{single} crack is the normalized SIFs for the case of a single crack. Moreover, the Ψ for tension loading, for example, is the ratio of the normalized SIFs for the case of two cracks with respect to normalized SIFs for the single crack case in tension loading. Thus, the following formula is utilized for this purpose:

$$\Psi > 1 + \Psi_c \quad (10)$$

$$\Psi < 1 - \Psi_c \quad (11)$$

Where Ψ_c is the critical or the tolerance value, which was set to 5%, based on Equation (9), there should be no interaction when Ψ=1. Therefore, Equation (10) represents the amplification effect, while the shielding effect is represented by Equation (11). Moreover, the values that lie in between the two limits are treated as isolated cracks. It should be noted that the same tolerance range or the critical value Ψ_c has been considered in [23]. Before any further work, it is essential to verify the validity of this finite element model. Then the stress intensity factor of the present model is compared with the existing results as in Table 1.

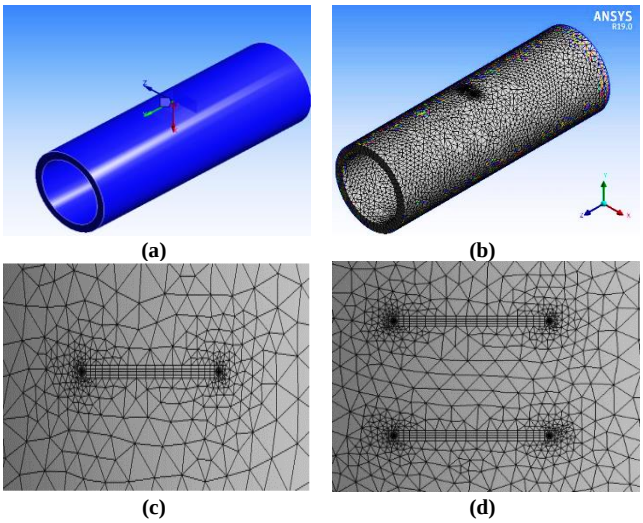

Fig. 2 Hollow cylinder with single crack (a) semi-elliptical crack setting, (b) overall cylinder mesh, (c) close to crack region, and (d) parallel cracks

4. Results and Discussion

4.1. Crack Interaction under Torsion Moment (Mode II)

The two parallel external cracks were examined under pure torsion loading, where $F_{Tor\text{-}II\text{–}EXT}$ and $F_{Tor\text{-}II\text{–}EXT}$ represent the normalized SIFs for modes II and III under torsion loading, respectively, since the mode I SIFs are absent. Therefore, Figures 3 and 4 show the normalized SIFs as a function of the normalized crack front position, $2\Theta/\pi$, for modes II and III, respectively. Figure 3 depicts the trend of $F_{Tor\text{-}II\text{–}EXT}$ when a/c=0.4, for a/t=0.2, 0.5 and 0.8. Maximum magnitude $F_{Tor\text{-}II\text{–}EXT}$ is attained at surface points A and C, while it gradually decreases until the approach to zero at the deepest point B on the crack front. Also, $F_{Tor\text{-}II\text{–}EXT,}$ in case of two cracks followed the same curve shape of $F_{\_SINGLE}$. The interaction influence has a direct proportion to the increase of a/t, where a notable crack interaction effect accompanied the relative crack depth increment.

Table 2 indicates the interaction factor Ψ for the two parallel cracks case under torsion in terms of mode II failure mode. Based on the distribution of $F_{Tor\text{-}II\text{–}EXT,}$ as shown in Figure 3, $F_{Tor\text{-}II\text{–}EXT}$ at the deepest point is equal to zero; therefore, it was not considered in Table 2. Also, Ψ results showed that under torsion loading, for mode II, the parallel cracks have a slight interaction influence on each other, which was clear by the shielding effect. Furthermore, the Ψ found to be similar at both A and C points, while the change in the separation distance between the cracks, s/L, produced an obvious impact, where for all examined a/t, small s/L produces high interaction influence, this is true until the two cracks deviated sufficiently, and each crack isolated from the other.

The maximum interaction influence was found when s/L=0.004 and a/t=0.8, about 37.6% reduction, while the minimum interaction effect for s/L=0.004 was found when a/t =0.2, about 23.1%.

Table 2. Interaction factor for parallel external cracks on thick cylinder under torsion mode II when a/c= 0.4

Point	a/t = 0.2			
	s/L=0.004	s/L=0.008	s/L=0.016	s/L=0.032
A	0.769	0.892	0.972	0.999
C	0.772	0.894	0.975	0.997
Point	a/t = 0.5			
	s/L=0.004	s/L=0.008	s/L=0.016	s/L=0.032
A	0.649	0.743	0.851	0.967
C	0.647	0.743	0.864	0.964
Point	a/t = 0.8			
	s/L=0.004	s/L=0.008	s/L=0.016	s/L=0.032
A	0.624	0.683	0.785	0.907
C	0.624	0.682	0.785	0.908

Table 3. Interaction factor for parallel external cracks on thick cylinder under torsion mode III when a/c= 0.4

Point	a/t = 0.2			
	s/L=0.004	s/L=0.004	s/L=0.004	s/L=0.004
A	0.881	0.961	0.997	1.005
B	0.870	0.958	1.007	1.008
C	0.884	0.966	1.001	1.006
Point	a/t = 0.5			
	s/L=0.004	s/L=0.004	s/L=0.004	s/L=0.004
A	0.541	0.838	0.997	1.037
B	0.805	0.873	0.970	1.028
C	0.543	0.846	1.000	1.042
Point	a/t = 0.8			
	s/L=0.004	s/L=0.004	s/L=0.004	s/L=0.004
A	-0.030	0.296	0.772	1.113
B	0.821	0.890	0.965	1.026
C	-0.018	0.300	0.770	1.117

4.2. Crack Interactions under Torsion Moment (Mode III)

Figure 4 reveals the distribution of mode III normalized SIFs under torsion loading for two external parallel cracks, $F_{Tor\text{-}III\text{–}EXT}$. As depicted by the graphs, $F_{Tor\text{-}III\text{–}EXT}$ is distributed along the crack front where the maximum value attained at the deepest point of the crack, point B, while $F_{Tor\text{-}III\text{–}EXT}$ at points A and C is always found to be less than that of point B. It should be noted that for each examined value of a/c, $F_{Tor\text{-}III\text{–}EXT}$ was calculated for three different values of a/t, 0.2, 0.5, and 0.8, for a single crack, $F_{\_SINGLE}$, was not affected by the change in the a/t, which means for such kind of cracks under torsion loading, the effect of change in crack depth on, $F_{Tor\text{-}III\text{–}EXT}$ was insignificant.

On the other hand, Table 3 shows the interaction factor Ψ for the external parallel cracks when a/c=0.4, for a/t=0.2, 0.5 and 0.8. Despite the presence of the maximum, $F_{Tor\text{-}III\text{–}EXT}$ at the deepest point on the crack front, the maximum Ψ attained at the surface points were found to be similar at A and C. Also, the maximum interaction influence has been found for s/L=0.004, which is similar to what has been seen for the previous loading types.

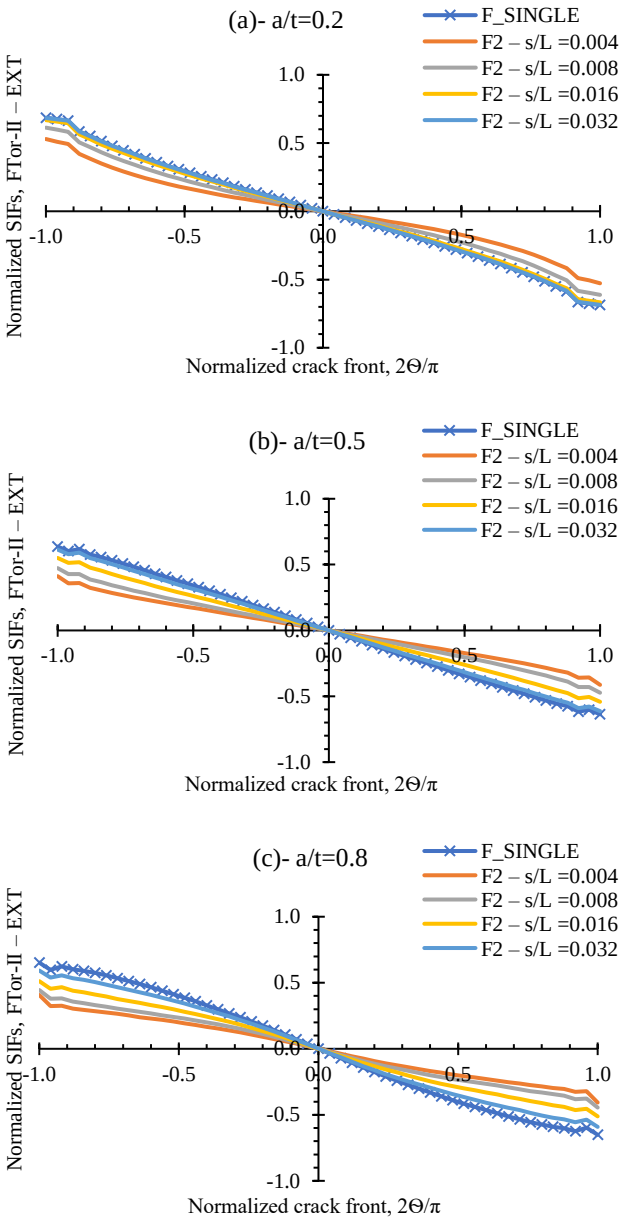

Fig. 3 The normalized SIFs for external parallel cracks under torsion mode II, for thick cylinder, a/c= 0.4, (a) a/t=0.2, (b) a/t =0.5, and (c) a/t=0.8

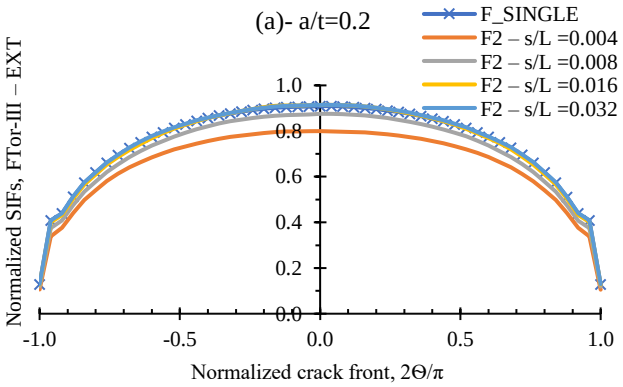

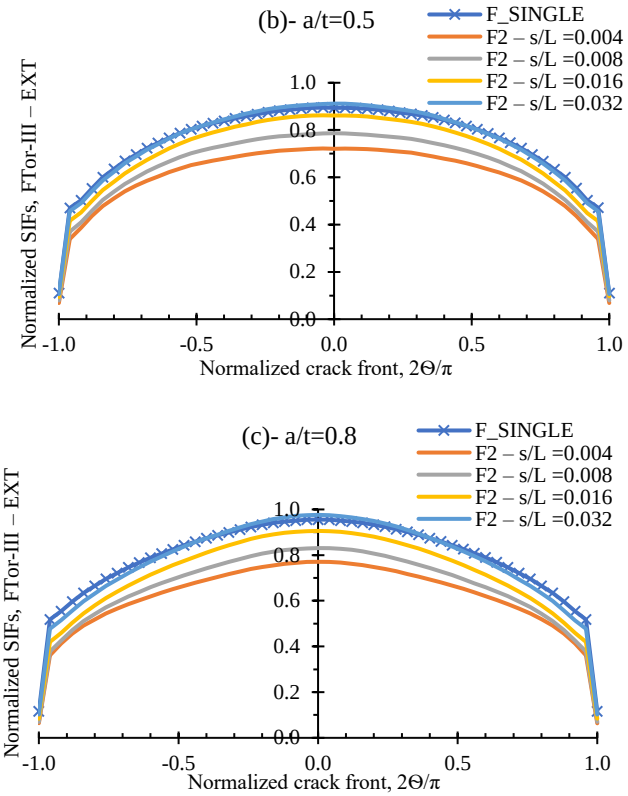

Fig. 4 The normalized SIFs for external parallel cracks under mode III torsions for thick cylinder, a/c=0.4, (a) a/t=0.2, (b) a/t =0.5, and (c) a/t=0.8.

Moreover, Ψ at A and C were 0.81, 0.62 and 0.55 for a/t=0.2, 0.5 and 0.8, respectively. This indicates that the crack depth has a significant impact on the interaction rate, where high a/t produced a high-level interaction effect and vice versa.

4.3. Crack Interactions under Combined Bending and Torsion Loading

The last examined type of loading on the external parallel cracks was the mixed mode loading, where a combination of tension and bending along with torsion were applied together on the thick cylinder. Different types of loading were used, and each type produced different modes of failure. Thus, the normalized SIFs for mixed mode loading were presented in terms of the equivalent SIFs, $F_{EQV-EXT}$, which was determined using Equation (7). Figure 5 illustrates the trend of $F_{EQV-EXT}$ for external parallel cracks when a/c=0.4, for a/t=0.2, 0.5 and 0.8. It can be inferred from the graphs that, for the same aspect ratio, a/c, the relative crack depth a/t, has a direct proportion with the value of $F_{EQV-EXT}$, where the change in a/t ratio produced a remarkable change in $F_{EQV-EXT}$.

Also, the distribution along the crack front of $F_{EQV-EXT}$ followed an identical manner to that of Tension and bending loading, where for low a/c, the trend was observed to be following a convex curve shape, while for high a/c, it was following a concave curve shape.

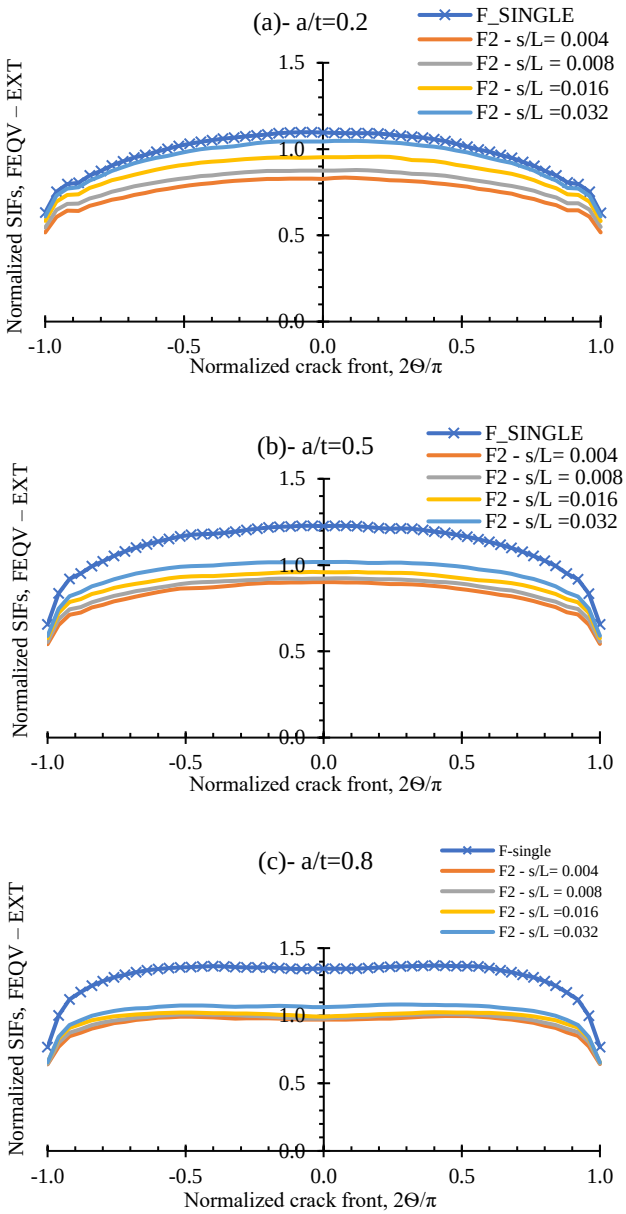

Fig. 5 The normalized SIFs for external parallel cracks under mixed mode for thick cylinder, a/c=0.4, (a) a/t=0.2, (b) a/t =0.5, and (c) a/t=0.8

This includes the predefined phenomenon, the transition effect, which has been explained earlier. In Table 4, the interaction factor Ψ, for external parallel cracks under combined loading for a/c=0.4 when a/t=0.2, 0.5 and 0.8 is presented.

Table 4. Interaction factor for parallel external cracks on thick cylinder under combined loading when a/c= 0.4.

Point	a/t = 0.2			
	s/L=0.004	s/L=0.004	s/L=0.004	s/L=0.004
A	0.821	0.870	0.924	0.968
B	0.755	0.799	0.870	0.954
C	0.817	0.862	0.923	0.965
Point	a/t = 0.5			
	s/L=0.004	s/L=0.004	s/L=0.004	s/L=0.004
A	0.826	0.847	0.879	0.899
B	0.735	0.752	0.782	0.830
C	0.824	0.844	0.879	0.898
Point	a/t = 0.8			
	s/L=0.004	s/L=0.004	s/L=0.004	s/L=0.004
A	0.838	0.843	0.854	0.853
B	0.721	0.727	0.737	0.789
C	0.833	0.838	0.852	0.852

It is obvious that based on the $F_{EQV-EXT}$ distribution along the crack front where the maximum value has been attained at the deepest point on the crack front, point B. Therefore, the maximum interaction influence is remarked at point B for all the examined a/t. Furthermore, the interaction impact increases with the increase of a/t. At the same time, this impact diminishes with the increase of the s/L value, which means that when the cracks are placed close to each other, this position enhances the interaction influence and vice versa. Also, cracks with high a/t require a large separation distance to be considered free from any other near-crack impact.

5. Conclusion

The distribution of the normalized SIFs along the crack front for double interacting surface cracks has been presented as a function of the normalized crack front position. Based on the examined crack orientations parallel, it is found that crack interaction could be in the form of amplification and shielding or no interaction. For parallel cracks, only shielding impact was noticed for all the examined crack geometrical parameters. The shielding impact found is an inverse proportion with the separation distance and the direct proportion between the shielding impact and the relative depth of the crack.

Acknowledgments

This research was supported by Universiti Tun Hussein Onn Malaysia (UTHM) through Tier 1 (vot. Q497).

References

[1] Ali Shaghaghi Moghaddam, Marco Alfano, and Rahmatollah Ghajar, "Determining the Mixed Mode Stress Intensity Factors of Surface Cracks in Functionally Graded Hollow Cylinders," *Materials & Design*, vol. 43, pp. 475-484, 2013. [CrossRef] [Google Scholar] [Publisher Link]

[2] Ali Fahem, Addis Kidane, and Michael A. Sutton, "Geometry Factors for Mode I Stress Intensity Factor of a Cylindrical Specimen with Spiral Crack Subjected to Torsion," *Engineering Fracture Mechanics*, vol. 214, pp. 79-94, 2019. [CrossRef] [Google Scholar] [Publisher Link]

[3] Kaige Zhu, Xiaodong Cui, and Daining Fang, "The Reinforcement and Defect Interaction of Two-Dimensional Lattice Materials with Imperfections," *International Journal of Solids and Structures*, vol. 49, no. 13, pp. 1908-1917, 2012. [CrossRef] [Google Scholar] [Publisher Link]

[4] Guozhong Chai, and Kangda Zhang, "Stress Intensity Factors for Interaction of Surface Crack and Embedded Crack in a Cylindrical Pressure Vessel," *International Journal of Pressure Vessels and Piping*, vol. 77, no. 9, pp. 539-548, 2000. [CrossRef] [Google Scholar] [Publisher Link]

[5] T.H. Leek, and I.C. Howard, "Estimating the Elastic Interaction Factors of Two Coplanar Surface Cracks Under Mode I Load," *International Journal of Pressure Vessels and Piping*, vol. 60, no. 3, pp. 307-321, 1994. [CrossRef] [Google Scholar] [Publisher Link]

[6] D.A. Pestov, A.A. Shamina, and A.V. Zvyagin, "Investigation of the Interaction of Rectangular Cracks by New Numerical Simulation Methods," *Acta Astronautica*, vol. 204, pp. 878-886, 2023. [CrossRef] [Google Scholar] [Publisher Link]

[7] Dong-Liang Sun, Xue-Yang Zhang, and Xian-Fang Li, "Interaction of Multiple Parallel Cracks in a Pre-Stressed Orthotropic Elastic Plane," *European Journal of Mechanics - A/Solids*, vol. 96, 2022. [CrossRef] [Google Scholar] [Publisher Link]

[8] Gérard Michot, "Mechanical Analysis of the Interaction between a Semi-Infinite Griffith Crack and its Coplanar Plastic Zone," *European Journal of Mechanics - A/Solids*, vol. 100, pp. 1-15, 2023. [CrossRef] [Google Scholar] [Publisher Link]

[9] Juha Kuutti, and Kari Kolari, "Interaction of Periodic Arrays of Wing Cracks," *Engineering Fracture Mechanics*, vol. 200, pp. 17-30, 2018. [CrossRef] [Google Scholar] [Publisher Link]

[10] Xiangqiao Yan, and Changing Miao, "Interaction of Multiple Cracks in a Rectangular Plate," *Applied Mathematical Modelling*, vol. 36, no. 11, pp. 5727-5740, 2012. [CrossRef] [Google Scholar] [Publisher Link]

[11] D. Ouinas et al., "Interaction Effect Crack–Interfacial Crack Using Finite Element Method," *Materials & Design*, vol. 31, no. 1, pp. 375-381, 2010. [CrossRef] [Google Scholar] [Publisher Link]

[12] K.J. Kirkhope, R. Bell, and J. Kirkhope, "Stress Intensity Factors for Single and Multiple Semi-Elliptical Surface Cracks in Pressurized Thick-Walled Cylinders," *International Journal of Pressure Vessels and Piping*, vol. 47, no. 2, pp. 247-257, 1991. [CrossRef] [Google Scholar] [Publisher Link]

[13] X.J. Zheng, A. Kiciak, and G. Glinka, "Weight Functions and Stress Intensity Factors for Internal Surface Semi-Elliptical Crack in Thick-Walled Cylinder," *Engineering Fracture Mechanics*, vol. 58, no. 3, pp. 207-221, 1997. [CrossRef] [Google Scholar] [Publisher Link]

[14] Chai Guozhong, Zhang Kangda, and Wu Dongdi, "Stress Intensity Factors for External Semielliptical Surface Cracks in Pressurized Thick-Walled Cylinders Using the Hybrid Boundary Element Method," *International Journal of Pressure Vessels and Piping*, vol. 64, no. 1, pp. 43-50, 1995. [CrossRef] [Google Scholar] [Publisher Link]

[15] Rahman Seifi, "Stress Intensity Factors for Internal Surface Cracks in Autofrettaged Functionally Graded Thick Cylinders Using Weight Function Method," *Theoretical and Applied Fracture Mechanics*, vol. 75, pp. 113-123, 2015. [CrossRef] [Google Scholar] [Publisher Link]

[16] C.L. Tan, and M.L. Shim, "Stress Intensity Factor Influence Coefficients for Internal Surface Cracks in Thick-Walled Cylinders," *International Journal of Pressure Vessels and Piping*, vol. 24, no. 1, pp. 49-72, 1986. [CrossRef] [Google Scholar] [Publisher Link]

[17] Jae-Min Gim, Ji-Su Shin, and Yun-Jae Kim, "Reference Stress Based J Estimation Formula for Cracked Cylinders with a Wide Range of Radius-to Thickness Ratios: Part II- Circumferential Surface Cracks," *International Journal of Pressure Vessels and Piping*, vol. 187, 2020. [CrossRef] [Google Scholar] [Publisher Link]

[18] Iman Eshraghi, and Nasser Soltani, "Stress Intensity Factor Calculation for Internal Circumferential Cracks in Functionally Graded Cylinders Using the Weight Function Approach," *Engineering Fracture Mechanics*, vol. 134, pp. 1-19, 2015. [CrossRef] [Google Scholar] [Publisher Link]

[19] I.V. Varfolomeyev, M. Petersilge, and M. Busch, "Stress Intensity Factors for Internal Circumferential Cracks in Thin- and Thick-Walled Cylinders," *Engineering Fracture Mechanics*, vol. 60, no. 5-6, pp. 491-500, 1998. [CrossRef] [Google Scholar] [Publisher Link]

[20] X.J. Zheng, G. Glinka, and R.N. Dubey, "Calculation of Stress Intensity Factors for Semielliptical Cracks in a Thick-Wall Cylinder," *International Journal of Pressure Vessels and Piping*, vol. 62, no. 3, pp. 249-258, 1995. [CrossRef] [Google Scholar] [Publisher Link]

[21] V. Caf, ANSYS Mechanical APDL Fracture Analysis Guide, 2019. [Online]. Available: https://www.scribd.com/document/626512324/ANSYS-Mechanical-APDL-Fracture-Analysis-Guide

[22] Y. Murakami, and S. Nemat-Nasser, "Interacting Dissimilar Semi-Elliptical Surface Flaws Under Tension and Bending," *Engineering Fracture Mechanics*, vol. 16, no. 3, pp. 373-386, 1982. [CrossRef] [Google Scholar] [Publisher Link]

[23] Samsol Faizal Anis et al., "Simplified Stress Field Determination for an Inclined Crack and Interaction between Two Cracks under Tension," *Theoretical and Applied Fracture Mechanics*, vol. 107, 2020. [CrossRef] [Google Scholar] [Publisher Link]